

Integrated physical detection technology in complicated surface subsidence area of mining area

LI Zhen tao (李振涛)¹, LI Quan ming (李全明)^{1,2,*}, ZHANG Hong (张红)²

¹China Academy of Safety Science & Technology, Key Laboratory of Safety Production of State Administration of Production Safety Supervision and Administration - Disaster Prevention Laboratory in Mine Goal, Beijing 100012

²North China Institute of Science & Technology, Sanhe, China

*Corresponding author: LI Quan-ming, liqm@casst-tec.com

Abstract

The geological conditions of the surface subsidence area in a mine are highly complex, so it is difficult to obtain accurate survey results by a single geophysical prospecting method. In this study, a high-density resistivity method and shallow seismic reflection method were used to detect the surface subsidence area in a mine in Shandong, China. Anomalies in subsidence, unknown voids, and groundwater present in the surface rock and soil body in the subsidence area were identified and analyzed by drilling. The proposed geophysical prospecting method provided high-resolution, visually rich images of the surface subsidence area of the mine. The activity of underground water plays a key role in surface collapse, so the results of this study may provide a workable scientific basis for the prevention of late surface subsidence disasters.

Keywords: Drilling; ground subsidence; high-density electrical method; 3D seismic.

1. Introduction

With the continuous expansion of underground mining, the increasing depth of mining, and the existence of underground karst geology, surface subsidence in mining areas is becoming a more serious geological threat. The surface subsidence caused by mine disturbances and karst geology are common dangers (HU Bingnan *et al.*, 2017). The mining process forms continuous subsidence basins on the surface in the absence of ground cracks, step-like sinking, collapse pits, or other discontinuous collapse phenomena as the destruction of the surface construction (structure) is controlled. Karst collapse can suddenly occur under complex conditions, generally a discontinuous collapse pit, on the surface of the mining structure (WANG Mingli, 2014). Ground surface collapse may severely harm ground engineering buildings, farmland, and roads. Collapse may even lead to casualties or other serious threats to the safety of nearby residents.

Comprehensive physical detection technology involves multiple geophysical methods for integrated geophysical exploration of the given detection area. The advantages of multiple geophysical methods can be combined to ensure high detection accuracy and reliable detection results. Worldwide, researchers have used physical detection techniques to engineer various

geological exploration processes. Geophysical methods are widely applied to mine detection (Cheng Jiulong *et al.*, 2014; Liu Shengdong *et al.*, 2014) and are typically very successful. Da Qianwei *et al.* (2012) and Hu Yunbing *et al.* (2006) applied a high-density electrical method to study 3D inversion and detection accuracy. Xi Zhenzhu *et al.* (2010) and Liang Shuang *et al.* (2003) used the transient electromagnetic method to detect formation structures. Gan Fuping *et al.* (2005) used shallow seismic reflection wave and refracted wave methods to detect karst geology. Peng Suping *et al.* (2002) used a seismic CT exploration method to assess coal mine top coal caving faces. Liu Jinghua *et al.* (2005) integrated a high-density electrical method, transient electromagnetic method, and radioactive soil enthalpy method to assess abnormal areas in goafs and subsidence areas in coal mining and subsidence areas. Sargent *et al.* (2009) used ultra-shallow three-dimensional reflection seismic technology to detect underground settlement caused by the dissolution of gypsum. The researchers confirmed the effectiveness of ultra-shallow seismic exploration technology in the detection of underground caverns. Ran *et al.* (2010) used an ultra-shallow 3D seismic exploration technique with a dense detector arrangement to reinforce steel buried near the ground surface. At present, geophysical exploration is mainly used to detect subsidence areas. Available

methods mainly include high-density electric, transient electromagnetic, geological radar detection, and shallow seismic reflection methods.

The high-density electrical method is an advanced direct current prospecting technology which is efficient, low-cost, and provides rich information. However, it functions only at limited detection depths (YANG Jingming,2012). Three-dimensional seismic exploration technology provides comprehensive information, high resolution, and high imaging accuracy. It can intuitively reflect fluctuations in the formation interface, but it is costly and altogether inefficient (SHI Zhanjie *et al.*,2013). In the present study, we adopted two integrated geophysical methods-the high-density electrical method and seismic reflection method-to assess the potential for surface collapse due to shallow karst topography and surface subsidence in a deep mine in Shandong, China.

2. Comprehensive surface subsidence area detection method

2.1 High-density electrical method

The high-density electrical method is an advanced direct current prospecting technology which combines electrical depth and profile measurements as a multi-device and multi-pole method., The resistivity law of underground geomaterials in 2D space can be observed by establishing an underground stable current field based on the differences in electrical properties between karst and surrounding rock. Underground geologic structures and inhomogeneous electrical properties can then be identified accordingly. The detection principle is shown in Figure 1.

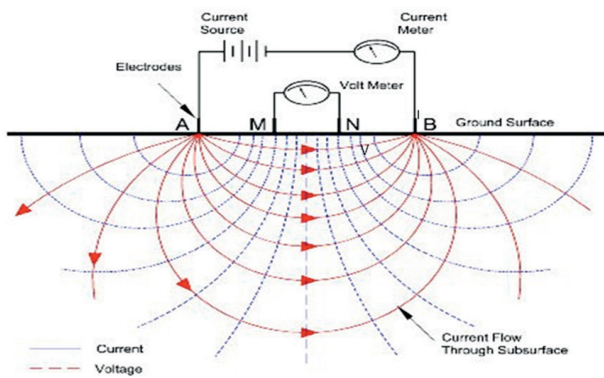


Fig. 1. Principle of high-density electrical detection.

Apparent resistivity is a parameter which reflects changes in karst and surrounding rock electrical

conductivity. It is mainly affected by the uneven distribution of electrical properties in the underground rock and the unevenness at its surface. The actual measured resistivity of the high-density electrical method is not true to the karst or surrounding rock. In fact, the value is actually the apparent resistivity. The general formula is as follows:

$$\rho_s = K \frac{\Delta U_{mn}}{I}$$

where I is the A, B power supply electrodes to the ground emission current, ΔU_{mn} is the M, N measurement of the primary field potential difference between the electrodes, $V \rho_s$ is the apparent resistivity, and $\Omega \cdot m K$ is the electrode device coefficient. Different measuring device electrodes have different coefficients (A Fa-you,2008).

The high-density electrical method is based on vertical direct current sounding, electrical profiles, and resistivity tomography. Its rolling scanning measurement not only provides rich geoelectricity information and improves the electrical resolving power, but also reduces man-made influencing factors and can markedly enhance efficiency. Its electrode arrangement and observation point distribution are shown in Figure 2.

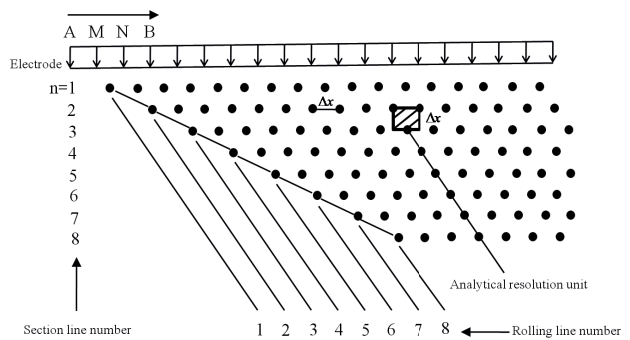


Fig. 2. High-density electrical method: Electrode arrangement and observation point distribution.

2.2 Three-dimensional seismic exploration

Three-dimensional seismic exploration involves various high-density forms of area observation systems, which are also known as area exploration methods. According to the propagation mode of seismic waves, shallow seismic exploration can be conducted using the following methods: shallow refracted wave, shallow reflection wave, surface wave, transmitted wave method (direct wave method), and seismic multiwave. See Figure 3.

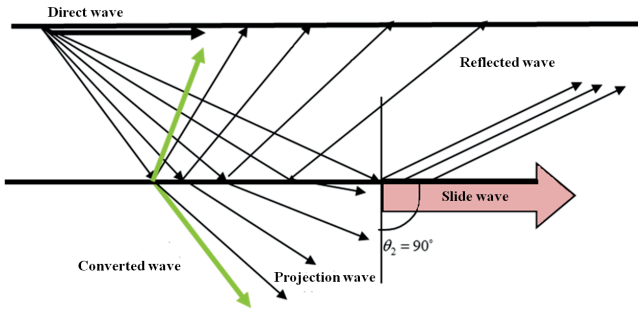


Fig. 3. Various seismic waves related to seismic exploration.

Three-dimensional seismic exploration utilizes the principle of artificially excited seismic waves to generate reflections at the rock-soil interface. This allows the detection of shallow stratum or structures with varying wave impedances. There are two types of reflection wave methods (single coverage and multiple coverage). According to the number of measurements of each reflection point on the reflective interface. The single-coverage observation system only measures one reflection point on the reflection interface, as shown in Figure 4. The multiple coverage observation system makes multiple reflections on each reflection point on the reflection interface (Figure 5).

We ran a 3D seismic survey field test to fully assess the stratum of the survey area, maximum exploration depth, dip of the stratum, rock velocity of the stratum, dynamic characteristics of the reflected wave, and other necessary information prior to our experiment. The results are shown in Figure 6.

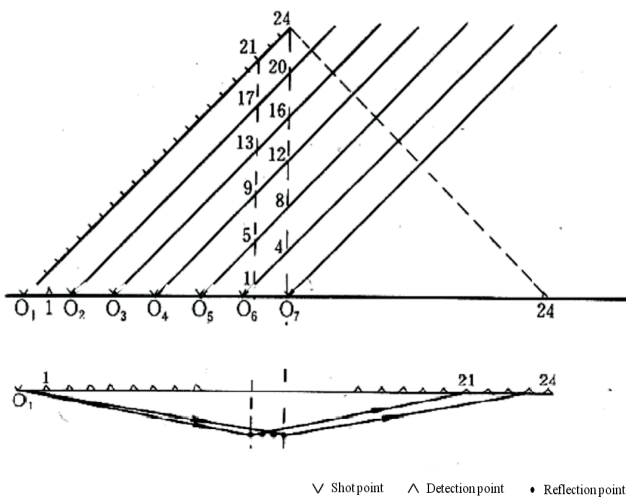


Fig. 4. Single cover observation system and diagram.

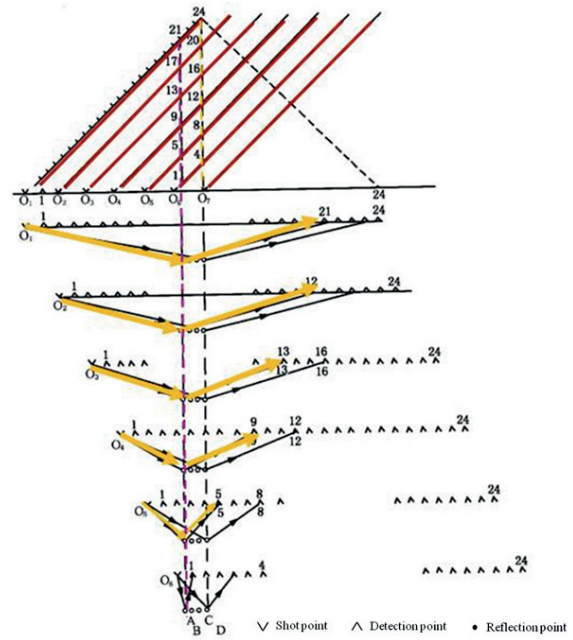


Fig. 5. Multiple coverage observation system and diagram (six-area coverage).

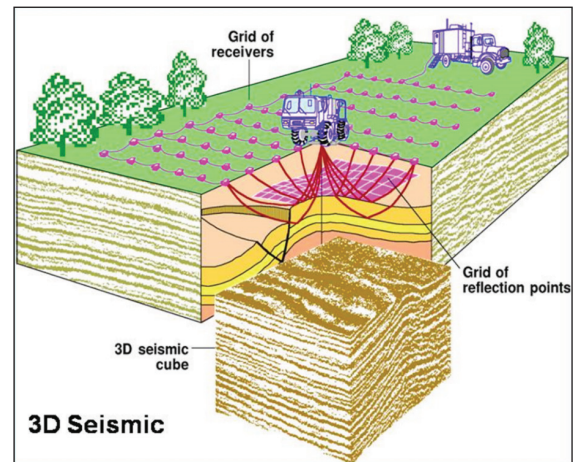


Fig. 6. Field layout of 3D seismic survey line.

3. Surface subsidence identification in mining area

Surface subsidence in a mining area is mainly caused by the underground mining process and underground karst medium. There are hidden collapse pits and unknown pits in the goafs and underground karst media formed by the mining process which are primarily responsible for surface subsidence. The goafs formed by underground mining destroy the original geological stability system in the ground and cause a loss of groundwater. The caves and collapse columns in the strata of mining areas are prone to karst collapse, column collapse, and other dangerous phenomena due to the influence of groundwater that may lead to surface collapse. The existence of goafs or hidden

collapse pits due to ground subsidence in the mining area “overburdens” the mine, or creates the “three-belt” structure shown in Figure 7.

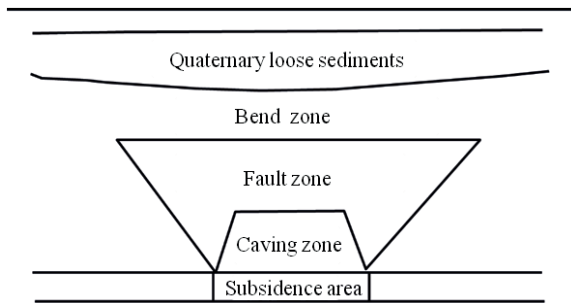


Fig. 7. Vertical three-belt structure due to surface subsidence of the mining area.

The high-density electrical method reveals abnormal resistance regions in the mine based on the plotted iso-receptivity contour map and inversion results. It informs the engineer of exactly the opposite of whether the caverns and the goafs contain water in the geoelectrical profile. If the water-free state is dry, the caverns and goafs are characterized by high resistivity; conversely, if water is present, the caverns and goafs are characterized by low resistivity. Before the goaf, cavern-bursting zone, and the collapse zone reach stability, their electrical resistivity changes with the degree of stability (Liu Jinghua *et al.* 2005) The common resistivity of ores, minerals, and various natural waters are shown in Tables 1-3.

Table 1. Resistivity (dry state) of common ore rocks.

Igneous rock		Metamorphic rock		Sedimentary rock	
Rock name	Resistivity/ Ωm	Rock name	Resistivity/ Ωm	Rock name	Resistivity/ Ωm
Granite	$3 \times 10^2 - 10^5$	Lava	$100 - 5 \times 10^4$	Conglomerate	$2 \times 10^3 - 1 \times 10^4$
Granite porphyry	1.3×10^6	Gabbro	$1000 - 5 \times 10^6$	Sandstone	$1 - 6.4 \times 10^3$
Syenite	1.0×10^6	Basalt	1.3×10^5	Dolomite	$350 - 5 \times 10^3$
Diorite	1.0×10^5	Pegmatite	6.3×10^3	Marl	3-70
Porphyrite	3.3×10^3	Hornfels	6.0×10^7	Clay	1-100
Quartz porphyry	$300 - 9 \times 10^5$	Schist	$20 - 1 \times 10^4$	Alluvial soil	10-800
Quartz diorite	1.8×10^5	Marble	2.5×10^5	Sand	10-800
Diorite porphyry	2.8×10^4	Skarn	2.5×10^8	Solid shale	20-2000
Andesite	1.7×10^2	Quartzite	$10 - 2 \times 10^5$	Argillaceous porphyry	10-800
Gabbro porphyry	1.7×10^5	Tuff	1.1×10^5	Unfixed clay	20-1000
Goaf	∞	Goaf	∞	Goaf	∞

Table 2. Resistivity of common minerals.

$10^{-3} - 10^{-6} / \Omega\text{m}$	$10^{-3} - 1 / \Omega\text{m}$	$1 - 10^3 / \Omega\text{m}$	$10^{-3} - 10^6 / \Omega\text{m}$	$\geq 10^6 / \Omega\text{m}$
Bornite	Arsenopyrite	Stibnite	Ilmenite	Hornblende
Graphite	Galena	Bismuthinite	Cinnabar	Gypsum
Copper orchid	Hematite	Wolframite	Limonite	Rock salt
Magnetite	Binarite	Cassiterite	Hematite	Garnet
Pyrite	Pyrite	Hematite	Serpentine	Calcite
-	Chalcopyrite	Siderite	Sphalerite	Quartz
-	Molybdenite	Chromite	Chromite	Fluorite

Table 3. Resistivity of different natural waters.

Water name	Rain	River water	Groundwater	Mine water	Seawater	Salt water
Resistivity/ Ωm	≥ 100	0.1-100	≤ 100	1-10	0.1-10	0.1-1

Three-dimensional seismic exploration reveals the seismic wave field response per the difference in wave impedance in a given study area. The gob area or hidden collapse pit and its surrounding rock mass have a certain degree of wave impedance difference which causes a response in the seismic wave field. This response allows the engineer to identify delineated goafs or the boundary of the hidden collapse pits. In this study, we used forward software to simulate and analyze seismic wave field response characteristics, to theoretically obtain the acquisition parameters required for seismic exploration. This was done to identify the minimum width thickness of goafs or hidden collapse pits. It also helped to determine a reasonable observation system.

4. Project example

Due to its abundance of underground mineral resources, the mining area in Shandong Province has many goafs and large amount of groundwater. There have been

many surface subsidence accidents within the mine area. In November 2017, the surface farmland within the mining area collapsed; the collapse pit was 9 m in length, 6 m wide, and 6 m deep. Surrounding landfills were immediately disposed of the following December. The upper quaternary strata in the mining area are relatively thick, ranging from 156 to 230 m, and lacking corresponding geological and hydrological data, so an integrated geophysical exploration technique was used to detect the area near the collapse pit in order to analyze the cause of the collapse.

4.1 High-density electrical detection

We used a SuperSting R8/IP high-density electrical detection system (AGI, USA). We gathered measurements with a four-stage Wenner device in two replications. The site wiring parameters and relevant diagrams are shown in Table 4 and Fig. 8; the detection results are shown in Figure 9.

Table 4. High-density electrical wiring parameters.

No.	Electrode distance /m	Number of electrodes/ individual	Wiring direction	Wiring length /m	Note
Line 1	6	58	East and west	342 m	The 31st electrode is located in the center of the collapse area
Line 2	6	58	East and west	342 m	The 31st electrode is located 18m north of the collapse area
Line 3	6	82	North and south	486 m	The 35th electrode is located at the west edge of the collapse zone

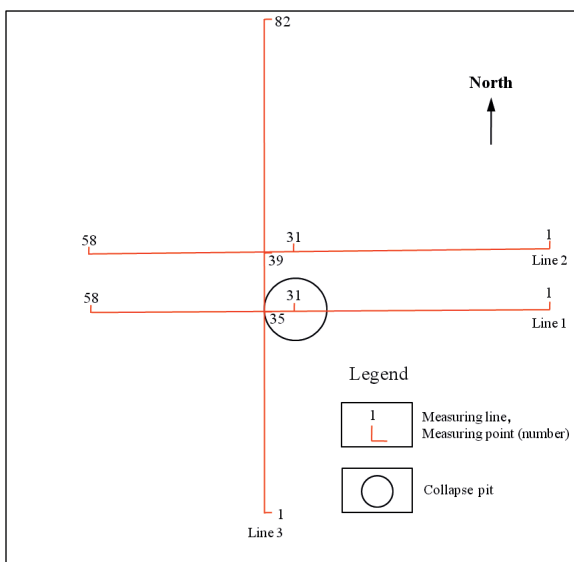


Fig. 8. Line layout.

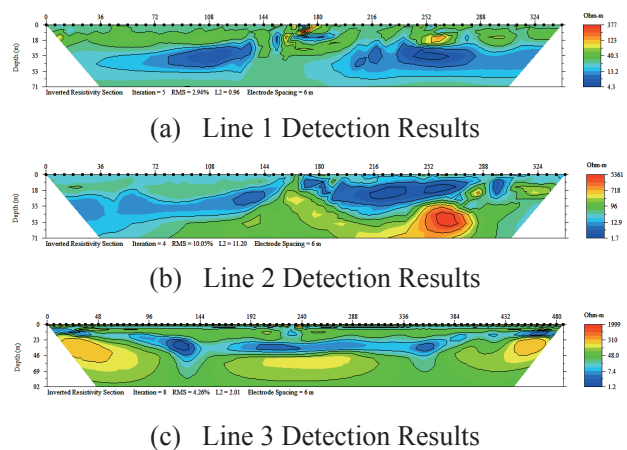


Fig. 9. High-density resistivity inversion of optic resistance profile.

The electric resistance of waste soil buried under the subsidence area of the survey line 1 is significantly higher

than that of the surrounding loess layer. There is an obvious low-resistance anomaly from 27 to 71 m deep on both sides, which may be an aquifer. Line 2, the area about 84 m away from the northwest of the collapse pit, is a high-resistance area which is presumed to be a sedimentary gravel layer; the rest is a low-resistance area which may be an aquifer. Line 3 is a low-resistance area with a depth of 12 to 21 m, which also may be an aquifer. There is a large area of low resistance below the subsidence area. It is presumed that there is a large quantity of ground water

in the subsidence area. There may be underground flow channels. In addition, there is no obvious high-resistance anomaly area present.

4.2 Three-dimensional seismic exploration

Through on-site testing, we conducted 3D seismic exploration on-site using wells with a depth of 4 m and doses of 1 kg and 10 Hz super detectors. The observation parameters are shown in Table 5, and the site layout is shown in Figure 10.

Table 5. Survey system parameters.

Receiving channel distance /m	Line distance /m	Excitation point spacing /m	Running distance /m	Surface element mesh (transverse x longitudinal)/ (m×m)
10	40	20	60	10×5



Fig. 10. Site layout of excitation and receiving points near collapse area.

According to the 3D seismic inline analysis of the collapsed area inline 669 (Figure 11) and the crossline 125 longitudinal section (the green arrow is the point of collapse in Figure 12), there is no significant velocity difference near the subsidence area. We observed changes from 0-250 m. From the depth of 85 m cross-sectional chromatographic data (Figure 13), there is no obvious speed change anomaly.

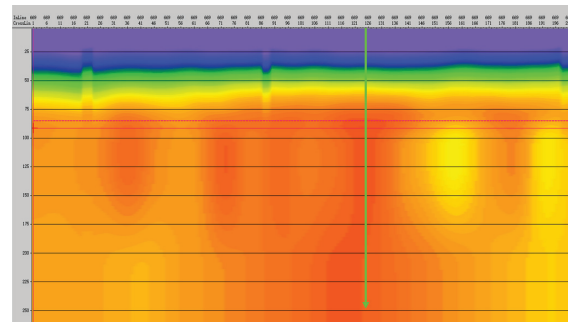


Fig. 12. Crossline 125 tomography data display.

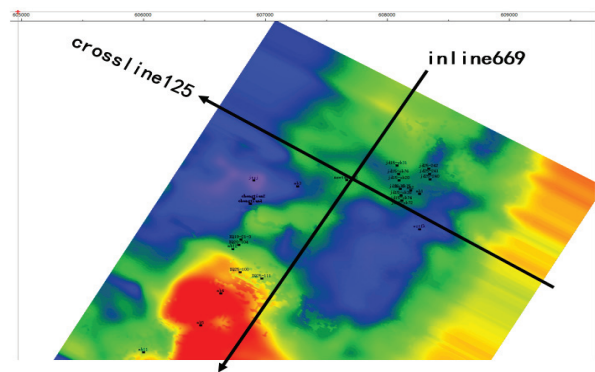


Fig. 13. Three-dimensional seismic data display near collapse area (depth 85 m, arrowhead intersection point is a collapse point).

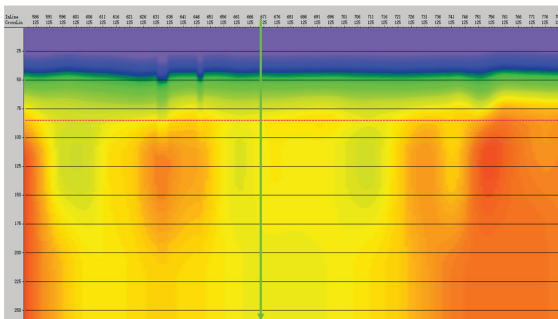


Fig. 11. Inline 669 tomography data display.

According to the longitudinal and lateral tomographic profiles of the 3D seismic data, no significant velocity change occurred at the collapse point or near it. No obvious void characteristics were observed within the range of 0 to 250 m at the collapse point and surrounding depth. The

chromatographic data level was based on a depth of 85 m. The subsidence point also did not show any obvious abnormal velocity change characteristics.

4.3 Drilling results analysis

We designed a drilling program according to the location and collapse depth of the farmland ground surface. We placed three boreholes in the subsidence area. The drilling parameters and schematics are shown in Figure 14.

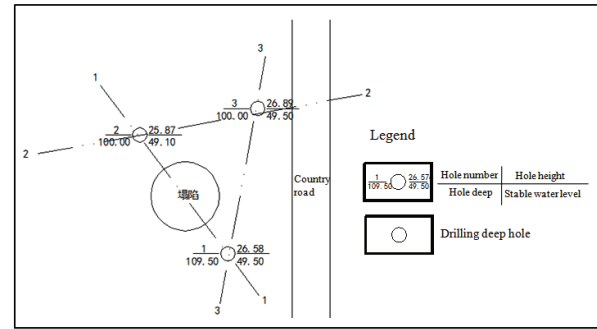


Fig.14. Position of the drill point plane

The drilling results are shown in Fig. 15 and Table 6.

Layer number	Bottom elevation (m)	Bottom depth (m)	Layered thickness (m)	Bar graph
1	26.08	0.50	0.50	▽▽▽▽
2	18.78	7.80	7.30	▽▽▽▽
3	2.08	24.50	16.70	▽▽▽▽
4	-21.42	48.00	23.50	▽▽▽▽
5	-26.42	53.00	5.00	z ▼
6	-29.42	56.00	3.00	▽▽▽▽
7	-41.42	68.00	12.00	cavity
8	-64.42	91.00	23.00	○ ○ ○ ○
12	-64.72	91.30	0.30	○ ○ ○ ○
13	-82.92	109.50	18.20	○ ○ ○ ○

Layer number	Bottom elevation (m)	Bottom depth (m)	Layered thickness (m)	Bar graph
1	25.37	0.50	0.50	▽▽▽▽
2	17.07	8.80	8.30	▽▽▽▽
3	2.87	23.00	14.20	▽▽▽▽
4	-17.14	43.00	20.00	▽▽▽▽
5	-26.14	52.00	9.00	z ▼
6	-39.14	65.00	13.00	▽▽▽▽
7	-42.14	68.00	3.00	○ ○ ○ ○
8	-46.14	72.00	4.00	○ ○ ○ ○
9	-56.14	82.00	10.00	○ ○ ○ ○
10	-62.64	88.50	6.50	Sm
11	-64.14	90.00	1.50	○ ○ ○ ○
12	-65.44	91.30	1.30	○ ○ ○ ○
13	-74.14	100.00	8.70	○ ○ ○ ○

Layer number	Bottom elevation (m)	Bottom depth (m)	Layered thickness (m)	Bar graph
1	26.39	0.50	0.50	▽▽▽▽
2	17.39	9.50	9.00	▽▽▽▽
3	1.89	25.00	15.50	▽▽▽▽
4	-20.11	47.00	22.00	▽▽▽▽
5	-26.11	53.00	6.00	z ▼
6	-37.61	64.50	11.50	▽▽▽▽
7	-41.11	68.00	3.50	○ ○ ○ ○
8	-43.11	70.00	2.00	○ ○ ○ ○
9	-55.11	82.00	12.00	○ ○ ○ ○
10	-61.11	88.00	6.00	Sm
11	-65.11	92.00	4.00	○ ○ ○ ○
12	-66.11	93.00	1.00	○ ○ ○ ○
13	-73.11	100.00	7.00	○ ○ ○ ○

(a) 1# drill hole columnar diagram (b) 2# drill hole columnar diagram (c) 3# drill hole columnar diagram

Fig.15. Drill hole columnar diagram.

Table 6. Stratigraphic characteristics in subsidence area.

Layer number	Name	Geotechnical description	Status	Buried depth/m
1	Cultivate soil	Brown, wet, and uneven soil, mainly clayey soil, containing a small amount of broken stones and a small amount of plant roots.	Loose	About 0.5
2	Silty clay	Gray brown-brown yellow, uniform soil, slightly smooth cut surface, slightly shiny, contains a small amount of iron and manganese oxide, dry strength and toughness is moderate, no shaking reaction, containing a small amount of bean ginger stone, particle size 3-5mm, content of about 5%, bottom contains ginger stone particle size of 5-10mm, content is 8%-10%.	Plastic	About 9.0
3	Silt	Gray-yellow, wet, rapid shaking response, rough cut surface, dull, low dry strength and low toughness, containing large amounts of iron and manganese oxides, small amount of mica pieces, bean-shaped ginger stone.	Plastic	About 24.0
4	Silty clay	Yellow, partly hard plastic, more uniform soil, slightly smooth cut surface, slight luster, moderate dry strength and toughness, no shaking reaction, containing large amounts of iron and manganese oxides, ginger stone size 5-30 mm, content 10%-30%.	Plastic	About 43.0
4-1	calicious nuts	Yellow, particle size 5-30 mm, content 60%-80%, calcareous cementation, short columnar core, hammer brittle, mixed with a lot of cohesive soil, clayey soil is hard plastic state, sublayer, distribution in west area, cementation thickness about 0.5 m.	Plastic	About 38.5
5	Medium-sized sand	Yellow, saturated, mineral composition is mainly quartz and feldspar, no sorting, no bedding, poor gradation, particle size larger than 0.25 mm accounted for 70% of the total mass, particles generally round, mixed with a lot of limestone pebbles.	Medium	About 52.0
5-1	Cemented conglomerate	Grayish-green gray, cements are mainly limestone pebbles, particle size of 10-50 mm diameter, roundness of particles is good, calcium cementation, cementation degree is medium, cementation length is 200-300 mm, drilling is difficult, hammer can be broken. Hammer is crushed and is soft rock, sub layer, distribution in west region, cement thickness about 0.5 m.	Dense	About 48.0
6	Silty clay	Yellow, more uniform soil, slightly smooth cut surface, slightly shiny, dry strength and toughness medium, no shake reaction, contains a lot of iron and manganese oxides, ginger size 5-30 mm, content of 20%-30%.	Stiff	About 64.0
7	Cobble	Gray-gray, saturated, the main rock composition is mainly limestone, sub-circular, particle roundness is good, poor sortability, non-layered, poor gradation, particle size is 10-50 mm, particle size greater than 20 mm accounts for about 60% of the total mass, filling material is medium sand.	Dense	About 68.0

Layer number	Name	Geotechnical description	Status	Buried depth/m
8	Cemented conglomerate	Gray-gray, cement is mainly composed of limestone pebbles, particle size is 10-50 mm, roundness of particles is good, calcareous cementation, cementation degree is medium cementation, drilling is difficult, hammering is crushed, it is soft rock.	Dense	约 72.0
9	Cobble	Gray-gray, saturated, the main rock composition is mainly limestone, sub-circular, particle roundness is better, poor sortability, non-layered, poor gradation, particle size is 10-50 mm, particle size greater than 20 mm accounts for about 80% of the total mass, filling material is medium sand.	Dense	About 82.0
10	Medium-sized sand	Yellow and saturated, mineral composition is mainly quartz and feldspar, no sorting, no bedding, poor gradation, particle size larger than 0.25 mm accounts for 70% of the total mass, particle are round, mixed with 10%-40% limestone and gravel pebbles.	Dense	About 88.0
11	Cobble	Gray-gray, saturated, rock composition is mainly limestone, sub-circular, particle roundness is better, poor sortability, non-layered, poor gradation, particle size is 10-50 mm, particle size greater than 20 mm accounts for about 80% of the total mass, filling material is medium sand.	Dense	About 92.0
12	Cemented conglomerate	Gray-gray, cement is mainly composed of limestone pebbles, particle size is 10-50 mm, roundness of particles is good, calcareous cementation, cementation degree is medium, drilling is difficult, hammering is crushed, it is soft rock.	Dense	About 93.0
13	Cobble	Gray-gray, saturated, main rock composition is limestone, sub-circular, particle roundness is better, poor sortability, non-layered, poor gradation, particle size is 10-50 mm, particle size greater than 20 mm accounts for about 80% of the total mass, filling material is medium sand.	Dense	—

Note: 1# hole 7-11 layer is missing.

5. Conclusion

(1) Comprehensive geophysical methods are superior to single geophysical methods in the detection of complex surface subsidence areas in mines. These methods allow for very effective extraction of geological information and are convenient, intuitive, and rich in data; however, their accuracy and efficiency merits further improvement per comprehensive interpretation of geophysical prospecting results and by comparison against drilling results. Integrated geophysical methods are better suited to the exploration of surface subsidence in mining areas. Geophysical methods can be combined based on the geological conditions at hand to avoid any interpretation bias caused by variations in geophysical results.

(2) In this study, we combined geophysical exploration and on-site drilling analysis. It was found that when the thickness of the overlying quaternary strata in the mining area was relatively large, the correlation between the mined-out area formed by underground mining and surface subsidence is not significant. Groundwater plays a key role in the formation of surface subsidence in the mining area.

(3) We ran a comprehensive geophysical prospecting and field drilling verification at a Shandong mining area. The hole and the abnormal area below the mining subsidence area may be attributable to the pumping of groundwater initially having caused 7, 9, 11 layers of sand drain. The eighth layer of cemented conglomerate is thin

and the effective protection of the upper part of the system inadequate, resulting in the collapse of the lower sand soil and aberrant development of the soil and, ultimately, to collapse of the surface.

References

- A Fa-you. (2008).** Application of High density Resistivity Method and Ground Penetrating Radar to Surveying Fault and Karst Caverns. Guiyang: Guizhou University. Pp. 12.
- Bachrach r & Reshef m. (2010).** 3D ultra shallow seismic imaging of buried pipe using dense receiver array: Practical and theoretical considerations. *Geophysice*, **75**(6): 45-51.
- Cheng Giulong, Li Fei, Peng Suping & Sun Xiaoyun. (2014).** Research progress and development direction on advanced detection in mine roadway working face using geophysical methods. *Journal of China Coal Society*, **39**(8): 1742-1750.
- Dai Qianwei, Xiao Bo & Feng Deshan. (2012).** 3-D inbersion of high density resitibity method based on 2-D exploration data and its application. *Journal of Central South University (Science and Technology)*, **43**(01): 293-300.
- Gan Fuping, Ma Zulu & Yu Liping. (2005).** Study on the application of shallow seismic method under complex conditions in karst area. *Journal of Geology and Exploration*, **5**(41): 75-78.
- Hu Bingnan, Jiang Zhongle & Guo Wenyan. (2014).** Temporal and spatial analysis of surface collapses factors in Qujiang Mine. *Journal of Coal Science and Technolgy*, **45**(1): 189-193.
- Hu Yunbing, Wu Yanqing, Song Jing & Kang Houqing. (2006).** Simulation model and example analysis of two dimensional electrical methods for detecting mined out area. *Journal of Mining Safety and Environmental Protection*, **6**(33): 39-41.
- Liang Shuang & Li Zhimin. (2003).** Analysis of the effect of the incidentally geomagnetic method in the exploration of the goaf in the two mine in Yangquan, *Journal of Coal Geology and Exploration*, **31**(4): 49-51.
- Liu Jinghua, Wang Zhuwen, Zhu Shi, Weng Aihua & Xia Anying. (2005).** Geophysical exploration of coal mine goaf and subsided area. *Journal of China Coal Society*, **12**(30): 715-719.
- Liu Shengdong, Liu Jing & Yue Jianhua. (2014).** Development status and key problems of Chinese mining geophysical technology. *Journal of China Coal Society*, **39**(1): 19-25.
- Peng Suping, Ling Biaocai & Liu Shengdong. (2002).** Application of seismic CT detection technology in fully mechanized top coal caving working face. *Journal of Rock Mechanics and Engineering*, **221**(12): 1786-1790.
- Sargent c & Goulty n. (2009).** Use of 3D seismic to image subsurface foundering due to gypsum dissolution. *First Break*, **27**: 61-67.
- Shi Zhanjie, Tian Gang, Zhao Wenke & Wang Zhihua. (2013).** Application of super shallow 3D seismic exploration technology. *Journal of Zhejiang University (Engineering Edition)*, **47**(5): 912-917.
- Wang Mingli. (2014).** Analysis on karst cover collapsing mechanism caused by underground coal mining. *Journal of Coal Science and Technolgy*, **42**(8): 5-8.
- Xi Zhenzhu, Liu Jian, Long Xia & Hou Haitao. (2010).** Three-component easurement in transient electromagnetic method. *Journal of Central South University (Science and Technology)*, **41**(01): 272-276.
- Yang Gingming. (2012).** Investigation effect of high density resistivity method in coal mine goaf. *Journal of Geophysical Prospecting and Geochemical Exploration*, **36** (S1): 12-15.

Submitted : 26/04/2018

Revised : 24/06/2018

Accepted : 27/06/2018

تقنية متكاملة للكشف الفيزيائي في مناطق هبوط السطح أثناء عملية التعدين

لي تشن تاو،^{1,2} لي تشيوان مينغ،² زانغ هونغ

¹الأكاديمية الصينية لعلوم وتكنولوجيا السلامة، المختبر الرئيسي لإنتاج السلامة في الإدارة العامة للإشراف على سلامة

الإنتاج وإدارته - مختبر الوقاية من الكوارث، بكين، الصين

²معهد شمال الصين للعلوم والتكنولوجيا، سانهي، الصين

الملخص

تعتبر الظروف الجيولوجية لمنطقة هبوط السطح في المنجم معقدة للغاية؛ ومن الصعب الحصول على نتائج مسح دقيقة باستخدام طريقة استكشاف جيوفيزيائية واحدة. في هذه الدراسة، تم استخدام طريقة مقاومة عالية الكثافة وطريقة الانعكاس الزلزالي الضحلة للكشف عن منطقة هبوط السطح في منجم في شانغونغ، الصين. تم تحديد وتحليل الحالات الشاذة في الهبوط، الفراغات غير المعروفة، والمياه الجوفية الموجودة في الصخور السطحية وجسم التربة في منطقة الهبوط عن طريق الحفر. قدمت طريقة التنقيب الجيوفيزيائية المقترحة صوراً عالية الدقة غنية بصرياً لمنطقة هبوط السطح في المنجم. يلعب نشاط المياه الجوفية دوراً رئيسياً في انهيار السطح، وبالتالي فإن نتائج هذه الدراسة توفر أساساً علمياً عملياً للوقاية من كوارث هبوط السطح.